Supplementary Material

Regioselective Atomic Layer Deposition in Metal-Organic Frameworks Directed by Dispersion Interactions

Leighanne C. Gallington,[1] In Soo Kim,[2] Wei-Guang Liu,[3] Andrey A. Yakovenko,[1] Ana E. Platero-Prats,[1] Zhanyong Li,[4] Timothy C. Wang,[4] Joseph T. Hupp,[4] Omar K. Farha,[4,5] Donald G. Truhlar,[3] Alex B.F. Martinson,[2] Karena W. Chapman[1*]

[1] X-ray Science Division, Advanced Photon Source, Argonne National Laboratory, Argonne, Illinois 60439-4858, United States

[2] Materials Science Division, Argonne National Laboratory, Argonne, Illinois 60439, United States

[3] Department of Chemistry, Chemical Theory Center, and Supercomputing Institute, University of Minnesota, Minneapolis, Minnesota 55455-0431, United States

[4] Department of Chemistry, Northwestern University, Evanston, Illinois 60208-3113, United States

[5] Department of Chemistry, Faculty of Science, King Abdulaziz University, Jeddah, Saudi Arabia

[*] email: chapmank@aps.anl.gov

ALD reactor assembly.

A schematic of the assembly used to perform atomic layer deposition *in situ* is shown in Figure S1. A previously described cell designed for nonambient temperatures and variable gas atmospheres was utilized as the reaction chamber.[1] The reaction chamber was heated using resistive heating elements (not shown), with temperature monitoring and feedback provided by a thermocouple. Heat shields were mounted to the cell to improve temperature stability.

Delivery of the inert carrier/purge gas to the flow cell was regulated using mass flow controllers (not shown). Helium (3.5 cc/min) was used in lieu of nitrogen to eliminate extraneous scattering contributions. The reaction chamber was held at 1.5×10^{-3} torr during purges and reached 2.5×10^{-3} torr during precursor doses using an Alcatel dual roughing/turbo vacuum pump system. ALD precursors were loaded into specially designed Swagelok cylinders and connected to the helium line using Swagelok tees.

To reduce the amount of pyrophoric precursor released in the event of a system breach, pairs of manual valves connected by steel tubing ($V=0.33$ cm^3) were placed between the helium lines and precursor cylinders. Both valves were initially closed to isolate the cylinders from the rest of the assembly. To introduce restricted amounts of precursor, the valve adjacent to the precursor (valve A) was opened, allowing vapor from the precursor to fill the head space between the valves. This valve was closed to re-isolate the cylinder from the system. The vapor contained in the head space was then delivered to the reactor chamber by opening the valve adjacent to the helium line (valve B) to allow flow into the system. Use of this administrative control allowed for a maximum diethylzinc dose of 0.37 µmoles. A pressure gauge was installed downstream of the diethylzinc cylinder to monitor the pressure upstream of the flow cell reactor. The same protocol was used to deliver water vapor (0.42 µmoles/dose) to the system. To prevent release unreacted precursor from the vacuum exhaust, a filter containing hydroxyl-rich glass wool was placed before the pump, thus insuring conversion of diethylzinc to nonhazardous zinc oxide.

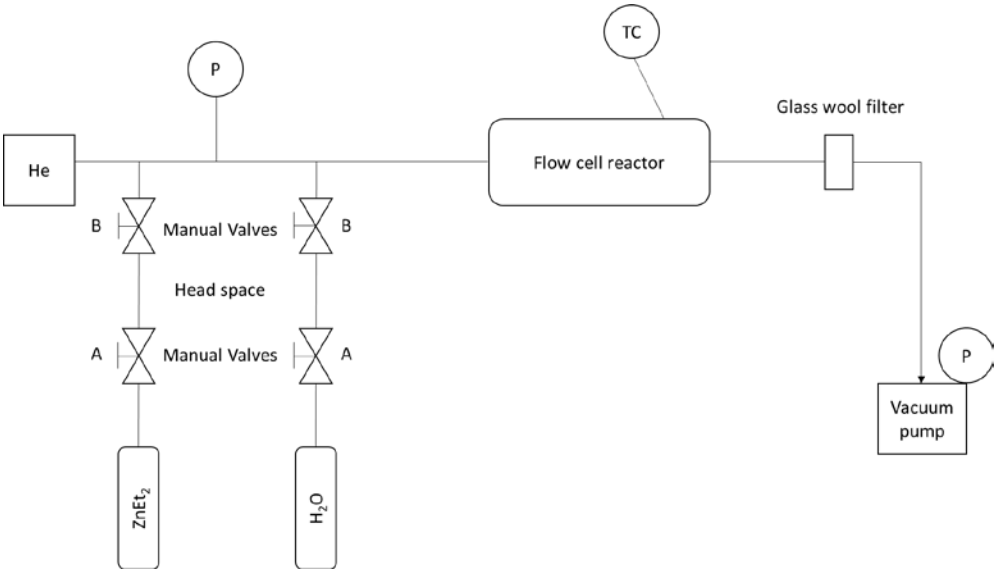

Figure S1 Schematic of ALD reactor. P denotes pressure gauge; TC denotes thermocouple. Components depicted in diagram are not to scale.

In situ synchrotron X-ray scattering measurements during AIM. Powder X-ray diffraction data suitable for difference envelope density analysis was collected at beamline 17-BM using an amorphous silicon based area detector (λ = 0.72768 Å). NU-1000 diluted with SiO_2 powder (~1:1) was loaded into a quartz capillary, which was then assembled into a flow cell reactor and mounted on the beamline. A nominal sample to detector distance of 1 m was used to allow for inclusion of low index peaks. Following standard ALD protocols for this system, the sample was pre-treated by heating at 125 °C under vacuum with He purge, hydrated with a single water dose, and allowed to equilibrate for 10 min. Powder diffraction data were collected following progressive dosing of (A) diethylzinc vapor and (B) water vapor at 125 °C. The dose sizes (on the order of 10^{-1} μmoles) were controlled by the volume of vapor contained in the spaces between two valves. Data were acquired over 4 full ALD cycles.

Analysis of powder diffraction data. Reduction of synchrotron powder diffraction images to one-dimensional patterns and calibration of sample to detector distance, beam center, tilt, and angular corrections were performed using GSAS-II.[2] Diffraction patterns were collected approximately 2 minutes after each dose. Lattice parameters and peak intensities were obtained from diffraction data via Le Bail whole pattern fitting.[3,4] A previously published crystal structure (P6/mmm) was used as a starting model for these analyses.[5] Lattice, profile, and Chebyshev polynomial background parameters were refined. A representative fit to data collected after 1 full ALD cycle is shown in Figure S2.

Difference envelope density analysis of powder diffraction data. Structure envelopes, surface boundaries which separate the high and low electron density regions of porous structures,[6,7] were calculated for each synchrotron powder diffraction dataset as previously described.[8,9] Ideal structure factors and phases were calculated from the NU-1000 crystal structure.[5,8] Structure envelope analyses typically make use of 1-10 low index reflections, as these peaks are generally well-separated with high scattering intensity, thereby allowing for accurate determination of integrated intensities. Due to the large size mismatch between the principal and hexagonal axes, inclusion of ~10 reflections provides limited resolution along the c axis (l_{max}=1) as compared with the hexagonal plane (h_{max}=4). To mitigate this, 24 reflections were chosen such that l_{max}=2 ({001} to {6-10}). Inclusion of higher index reflections (l_{max}=3) introduced a noticeable amount of noise into the analysis.

Difference envelope densities (DEDs) reflecting electron density added during the ALD process were calculated as previously described.[9] NU-1000 at 125°C before ALD was selected as the control structure envelope to insure that the difference envelope density map reflected changes induced by the deposition of zinc and subsequent water treatment as opposed to any changes due to heat treatment such as thermal expansion and node distortion. The structure envelope for this control was subtracted from appropriately scaled structure envelopes of datasets collected during ALD to generate the corresponding DEDs.[9] Surfaces were drawn at a cut-off level of 1.7σ above zero to insure that the DED maps preferentially reflect contributions from the strongest scatterer (Zn) over other scatterers such as organics and water.[10]

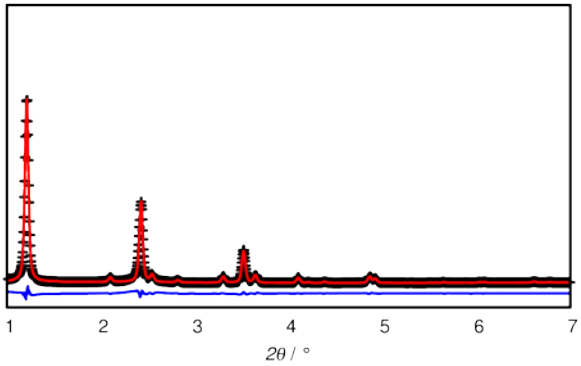

Figure S2 Representative Le Bail fit of P6/mmm model to PXRD data collected after one complete ALD cycle: observed data (black cross); calculated peak profile (red); difference curve (blue).

Structure optimization via density functional calculations. A geometry optimized model for NU-1000 was derived from the reported crystal structure[5] using the PBE-D2 or M06-L functional within CRYSTAL14.[11] Kohn-Sham density functional theory was used to evaluate the potential energy change associated with DEZ deposition on different node faces. Calculations were performed using the M06-L, PBE-D2, and PBE//PBE-D2 exchange-correlation functionals. First the structure was optimized. In the optimization, the 6-31G(d)[12] basis set was used for H, C and O; and the SDD effective core potential and corresponding basis set were used for Zr[13,14] and Zn[15] with exponents less than 0.06 removed. (The initial structure models were obtained by optimizing a cluster model containing one Zr_6–based node with eight formate linkers with the same level of basis sets used in the optimization of periodic structure at PBE level with the *Gaussian 09*[16] program; this was followed by coordinate transformation to the periodic cell and full optimization.) The structural optimization was followed by a single-point calculation with the larger basis set described in the article proper. The total number of atoms in the unit cell of NU-1000 (including $Zn(Et)_2$) is 603.

Quantification of inorganic content. Inductively coupled plasma-optical emission spectrometry (ICP-OES) was performed on an iCAP 6200 spectrometer (Thermo Fisher Scientific). Samples (< 1 mg) were recovered after atomic layer deposition and transferred to 25 mL volumetric flasks. 750 µL of sulfuric acid (99.999%) was added to each sample, followed by 250 µL of hydrogen peroxide solution (30 wt. %). The resulting solutions were gently sonicated until digestion was complete. 24 mL of deionized water (18.1 MΩcm) was added to each sample solution, which were further sonicated for 10 minutes.

Table S1 Lattice parameters of NU-1000 and Zn-AIM measured ex situ after 1 full ALD cycle.

	NU-1000	Zn-AIM
a (Å)	39.515(5)	39.998(3)
c (Å)	16.5224(19)	16.167(2)

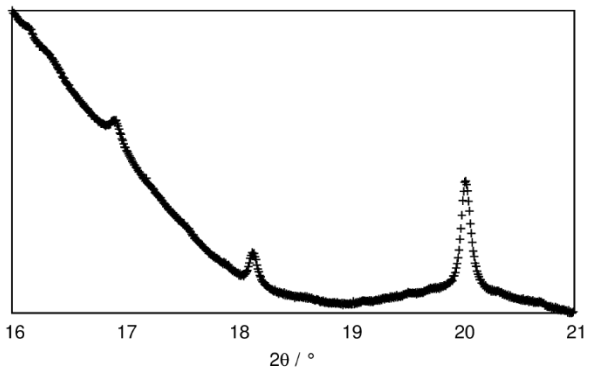

Figure S3 Powder x-ray diffraction pattern of NU-1000 after four full zinc oxide ALD cycles. Only the high angle region of the diffraction pattern is shown.

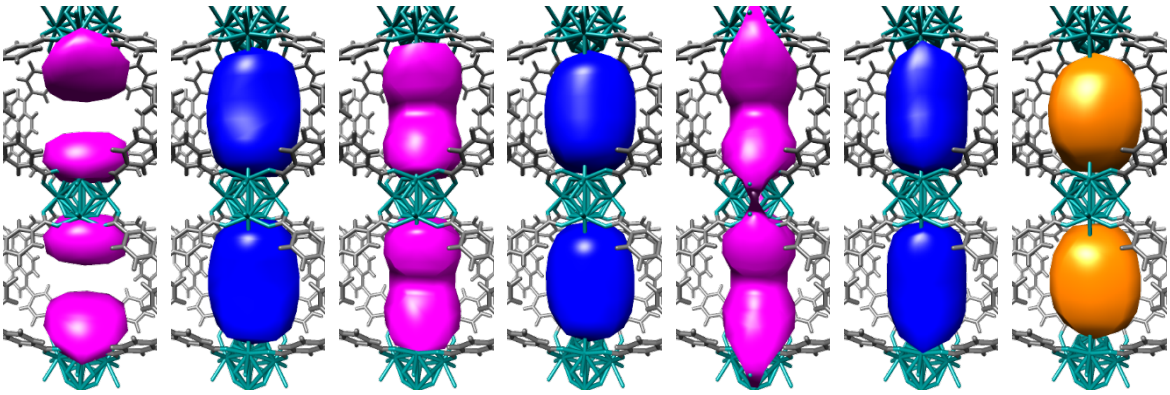

Figure S4 Difference envelope density maps of NU-1000 during atomic layer deposition of oxy-Zn(II) species viewed along c axis: (a) first A half cycle (b) first B half cycle (c) second A half cycle (d) second B half cycle (e) third A half cycle (f) third B half cycle (g) Zn-AIM examined ex situ after a full ALD cycle.

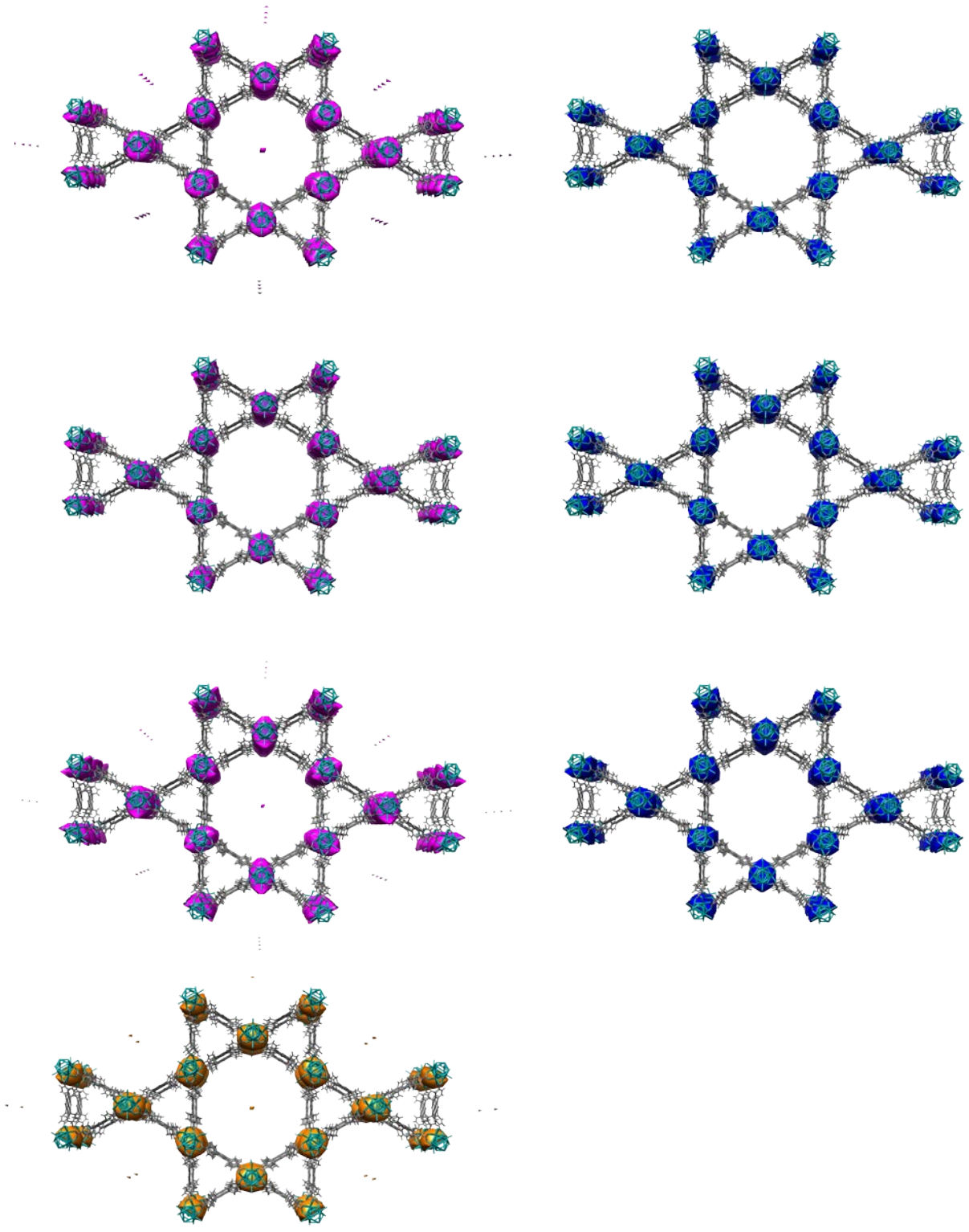

Figure S5 Difference envelope density maps of NU-1000 during atomic layer deposition of oxy-Zn(II) species viewed in a/b plane: (a) first A half cycle (b) first B half cycle (c) second A half cycle (d) second B half cycle (e) third A half cycle (f) third B half cycle (g) Zn-AIM examined ex situ after a full ALD cycle.

Effects of increased ligand size on preference for small pores.

The effect of dispersion can be even larger for additives with bulkier ligands than the $ZnEt_2$ considered here. For example, we made similar calculations for bis(N,N'-di-tert-butylacetamidinato)iron(II), which has the formula $C_{20}H_{42}N_4Fe$, as compared to $C_4H_{10}Zn$, and has been used as the ALD precursor to deposit Fe.[17] The reaction is:

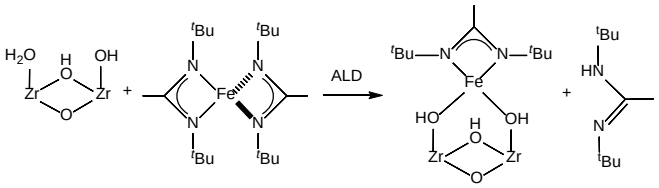

We found a preference of 9.2 kcal/mol for the product in the small pore, of which 7.0 kcal/mol was contributed by the D2 term.

Contents of selected SUPERFIP setup files (INFIP-format) used for generation of structure envelopes (calculated, NU-1000, and Zn-AIM).

NU-1000 (calculated from crystal structure)

```
title  EnvelopMaker parameters: nu1000 calculated ideal intesities:

# crystallographic data
#----------------------
cell    39.7867   39.7867   16.3173   90.0000   90.0000   120.0000

# spacegroup P6/mmm
spacegroup P6/mmm
centro yes
centers
  0.000000  0.000000  0.000000
endcenters
symmetry
     x1     x2     x3
    -x2  x1-x2     x3
 -x1+x2    -x1     x3
    -x1    -x2     x3
     x2 -x1+x2     x3
  x1-x2     x1     x3
     x2     x1    -x3
  x1-x2    -x2    -x3
    -x1 -x1+x2    -x3
    -x2    -x1    -x3
 -x1+x2     x2    -x3
     x1  x1-x2    -x3
    -x1    -x2    -x3
     x2 -x1+x2    -x3
  x1-x2     x1    -x3
     x1     x2    -x3
    -x2  x1-x2    -x3
 -x1+x2    -x1    -x3
    -x2    -x1     x3
 -x1+x2     x2     x3
     x1  x1-x2     x3
     x2     x1     x3
  x1-x2    -x2     x3
```

```
    -x1 -x1+x2     x3
endsymmetry

# Grid definition for density maps
#---------------------------------
dimension 3
voxel AUTO

# Control parameters for Superflip run
#---------------------------------
maxcycles 10000
repeatmode  1
bestdensities  1

outputfile nu1k_calc_11202015_6_-1_0.xplor
expandedlog yes

# Keywords for charge flipping
#---------------------------------
perform fourier
delta AUTO
weakratio 0.0
Biso 0.0
randomseed AUTO
searchsymmetry average

# Input Data
#---------------------------------

dataformat intensity phase
fbegin
#  h   k   l        F^2obs          phase
   1   0   0      7973.7100         0.5
   2  -1   0       451.4900         0.5
   2   0   0     10862.4700         0.0
   0   0   1      7001.1000         0.0
   1   0   1       735.5300         0.5
   2  -1   1      1322.3000         0.5
   2   0   1      9380.8600         0.0
   3   0   0      4638.1400         0.5
   3  -1   1      1347.5600         0.5
   4  -2   0        57.7000         0.0
   4  -1   0       471.1900         0.5
   3   0   1       103.3400         0.5
   4   0   0      5257.9400         0.0
   4  -2   1      2954.1100         0.0
   0   0   2       247.0000         0.5
   5  -2   0       139.2800         0.0
   2  -1   2       120.9800         0.5
   2   0   2       573.3100         0.0
   5  -2   1       246.4800         0.5
   3  -1   2       268.7100         0.5
   5   0   0      1578.7600         0.5
   6  -3   0       215.6900         0.5
   4  -2   2      1166.4800         0.0
   6  -1   0       515.4300         0.5
endf
```

NU-1000 (sample—pre-ALD)

```
title  EnvelopMaker parameters: nu1k_calc_11202015_6_-1_0.inflip intesities:
IC521_03.cif
# crystallographic data
#----------------------
cell    39.7867   39.7867   16.3173   90.0000   90.0000   120.0000

# spacegroup P6/mmm
spacegroup P6/mmm
centro yes
centers
  0.000000  0.000000  0.000000
endcenters
symmetry
     x1     x2     x3
    -x2  x1-x2     x3
 -x1+x2    -x1     x3
    -x1    -x2     x3
     x2 -x1+x2     x3
  x1-x2     x1     x3
     x2     x1    -x3
  x1-x2    -x2    -x3
    -x1 -x1+x2    -x3
    -x2    -x1    -x3
 -x1+x2     x2    -x3
     x1  x1-x2    -x3
    -x1    -x2    -x3
     x2 -x1+x2    -x3
  x1-x2     x1    -x3
     x1     x2    -x3
    -x2  x1-x2    -x3
 -x1+x2    -x1    -x3
    -x2    -x1     x3
 -x1+x2     x2     x3
     x1  x1-x2     x3
     x2     x1     x3
  x1-x2    -x2     x3
    -x1 -x1+x2     x3
endsymmetry

# Grid definition for density maps
#---------------------------------
dimension 3
voxel AUTO

# Control parameters for Superflip run
#---------------------------------
maxcycles 10000
repeatmode  1
bestdensities  1

outputfile IC521_03.xplor
expandedlog yes

# Keywords for charge flipping
#---------------------------------
```

```
perform fourier
delta AUTO
weakratio 0.0
Biso 0.0
randomseed AUTO
searchsymmetry average

# Input Data
#--------------------------------

dataformat intensity phase
fbegin
#  h   k   l        F^2obs          phase
   1   0   0      6368.4000         0.5
   2  -1   0       356.2000         0.5
   2   0   0     10000.0000         0.0
   0   0   1      4947.9000         0.0
   1   0   1       387.0000         0.5
   2  -1   1      1022.9000         0.5
   2   0   1      6633.1000         0.0
   3   0   0      2432.1000         0.5
   3  -1   1       733.6000         0.5
   4  -2   0       160.3000         0.0
   4  -1   0       326.7000         0.5
   3   0   1        46.2000         0.5
   4   0   0      3728.9000         0.0
   4  -2   1      1791.7000         0.0
   0   0   2       189.2000         0.5
   5  -2   0        86.0000         0.0
   2  -1   2       122.9000         0.5
   2   0   2       434.7000         0.0
   5  -2   1        92.5000         0.5
   3  -1   2       164.4000         0.5
   5   0   0       788.9000         0.5
   6  -3   0       127.9000         0.5
   4  -2   2       748.2000         0.0
   6  -1   0       284.7000         0.5
endf
```

Zn-AIM (in situ)

```
title  EnvelopMaker parameters: nu1k_calc_11202015_6_-1_0.inflip intesities:
IC521_26.cif
# crystallographic data
#----------------------
cell    39.7867   39.7867   16.3173   90.0000   90.0000   120.0000

# spacegroup P6/mmm
spacegroup P6/mmm
centro yes
centers
  0.000000  0.000000  0.000000
endcenters
symmetry
     x1     x2     x3
    -x2  x1-x2     x3
 -x1+x2    -x1     x3
```

```
    -x1    -x2     x3
     x2 -x1+x2     x3
  x1-x2     x1     x3
     x2     x1    -x3
  x1-x2    -x2    -x3
    -x1 -x1+x2    -x3
    -x2    -x1    -x3
 -x1+x2     x2    -x3
     x1  x1-x2    -x3
    -x1    -x2    -x3
     x2 -x1+x2    -x3
  x1-x2     x1    -x3
     x1     x2    -x3
    -x2  x1-x2    -x3
 -x1+x2    -x1    -x3
    -x2    -x1     x3
 -x1+x2     x2     x3
     x1  x1-x2     x3
     x2     x1     x3
  x1-x2    -x2     x3
    -x1 -x1+x2     x3
endsymmetry

# Grid definition for density maps
#---------------------------------
dimension 3
voxel AUTO

# Control parameters for Superflip run
#---------------------------------
maxcycles 10000
repeatmode  1
bestdensities  1

outputfile IC521_26.xplor
expandedlog yes

# Keywords for charge flipping
#---------------------------------
perform fourier
delta AUTO
weakratio 0.0
Biso 0.0
randomseed AUTO
searchsymmetry average

# Input Data
#---------------------------------

dataformat intensity phase
fbegin
#  h   k   l        F^2obs          phase
   1   0   0      5282.8000         0.5
   2  -1   0       520.2000         0.5
   2   0   0     10000.0000         0.0
   0   0   1      1871.3000         0.0
   1   0   1        78.6000         0.5
```

```
   2  -1   1       452.2000         0.5
   2   0   1      2453.4000         0.0
   3   0   0      1527.3000         0.5
   3  -1   1       281.3000         0.5
   4  -2   0       375.4000         0.0
   4  -1   0       274.1000         0.5
   3   0   1        11.9000         0.5
   4   0   0      2650.9000         0.0
   4  -2   1       498.0000         0.0
   0   0   2       125.6000         0.5
   5  -2   0        17.0000         0.0
   2  -1   2        35.3000         0.5
   2   0   2       173.8000         0.0
   5  -2   1         2.6000         0.5
   3  -1   2        54.0000         0.5
   5   0   0       340.0000         0.5
   6  -3   0         7.3000         0.5
   4  -2   2       281.4000         0.0
   6  -1   0       122.5000         0.5
endf
```

References

(1) Chupas, P. J.; Chapman, K. W.; Kurtz, C.; Hanson, J. C.; Lee, P. L.; Grey, C. P. *J. Appl. Crystallogr.* **2008**, *41*, 822.

(2) Toby, B. H.; Von Dreele, R. B. *J. Appl. Crys.* **2013**, *46*, 544.

(3) Le Bail, A.; Duroy, H.; Fourquet, J. L. *Mater. Res. Bull.* **1988**, *23*, 447.

(4) Petříček, V.; Dušek, M.; Palatinus, L. *Z. Kristallogr.* **2014**, *229*, 345.

(5) Mondloch, J. E.; Bury, W.; Fairen-Jimenez, D.; Kwon, S.; DeMarco, E. J.; Weston, M. H.; Sarjeant, A. A.; Nguyen, S. T.; Stair, P. C.; Snurr, R. Q.; Farha, O. K.; Hupp, J. T. *J. Am. Chem. Soc.* **2013**, *135*, 10294.

(6) McCusker, L. B.; Baerlocher, C.; Grosse-Kunstleve, R.; Brenner, S.; Wessels, T. *CHIMIA* **2001**, *55*, 497.

(7) Brenner, S.; McCusker, L. B.; Baerlocher, C. *J. Appl. Crys.* **1997**, *30*, 1167.

(8) Yakovenko, A. A.; Reibenspies, J. H.; Bhuvanesh, N.; Zhou, H.-C. *J. Appl. Crys.* **2013**, *46*, 346.

(9) Yakovenko, A. A.; Wei, Z.; Wriedt, M.; Li, J.-R.; Halder, G. J.; Zhou, H.-C. *Cryst. Growth Des.* **2014**, *14*, 5397.

(10) Chen, Y.-P.; Liu, Y.; Liu, D.; Bosch, M.; Zhou, H.-C. *J. Am. Chem. Soc.* **2015**, *137*, 2919.

(11) Dovesi, R.; Orlando, R.; Erba, A.; Zicovich-Wilson, C. M.; Civalleri, B.; Casassa, S.; Maschio, L.; Ferrabone, M.; De La Pierre, M.; D'Arco, P.; Noel, Y.; Causa, M.; Rerat, M.; Kirtman, B. *Int. J. Quantum Chem.* **2014**, *114*, 1287.

(12) Hehre, W. J.; Ditchfie.R; Pople, J. A. *J. Chem. Phys.* **1972**, *56*, 2257.

(13) Andrae, D.; Häußermann, U.; Dolg, M.; Stoll, H.; Preuß, H. *Theor. Chim. Acta* **1990**, *77*, 123.

(14) Martin, J. M. L.; Sundermann, A. *J. Chem. Phys.* **2001**, *114*, 3408.

(15) Dolg, M.; Wedig, U.; Stoll, H.; Preuss, H. *J. Chem. Phys.* **1987**, *86*, 866.

(16) Frisch, M. J.; Trucks, G. W.; Schlegel, H. B.; Scuseria, G. E.; Robb, M. A.; Cheeseman, J. R.; Scalmani, G.; Barone, V.; Mennucci, B.; Petersson, G. A.; Nakatsuji, H.; Caricato, M.; Li, X.; Hratchian, H. P.; Izmaylov, A. F.; Bloino, J.; Zheng, G.; Sonnenberg, J. L.; Hada, M.; Ehara, M.; Toyota, K.; Fukuda, R.; Hasegawa, J.; Ishida, M.; Nakajima, T.; Honda, Y.; Kitao, O.; Nakai, H.; Vreven, T.; Montgomery Jr., J. A.; Peralta, J. E.; Ogliaro, F.; Bearpark, M. J.; Heyd, J.; Brothers, E. N.; Kudin, K. N.; Staroverov, V. N.; Kobayashi, R.; Normand, J.; Raghavachari, K.; Rendell, A. P.; Burant, J. C.; Iyengar, S. S.; Tomasi, J.; Cossi, M.; Rega, N.; Millam, N. J.; Klene, M.; Knox, J. E.; Cross, J. B.; Bakken, V.; Adamo, C.; Jaramillo, J.; Gomperts, R.; Stratmann, R. E.; Yazyev, O.; Austin, A. J.; Cammi, R.; Pomelli, C.; Ochterski, J. W.; Martin, R. L.; Morokuma, K.; Zakrzewski, V. G.; Voth, G. A.; Salvador, P.; Dannenberg, J. J.; Dapprich, S.; Daniels, A. D.; Farkas, Ö.; Foresman, J. B.; Ortiz, J. V.; Cioslowski, J.; Fox, D. J.; Gaussian, Inc.: Wallingford, CT, USA, 2009.

(17) Avila, J. R.; Kim, D. W.; Rimoldi, M.; Farha, O. K.; Hupp, J. T. *ACS Appl. Mater. Interfaces* **2015**, *7*, 16138.